Nonlinear Development of Shocklike Structure in the Solar Wind

E. Lee,* G. K. Parks, M. Wilber, and N. Lin

Space Sciences Laboratory, University of California, Berkeley, California 94720, USA

(Received 24 February 2009; published 16 July 2009)

We report first *in situ* multispacecraft observations of nonlinear steepening of compressional pulses in the solar wind upstream of Earth's bow shock. The magnetic field of a compressional pulse formed at the upstream edge of density holes is shown to suddenly break and steepen into a shocklike structure. During the early phase of development thermalization of ions is insignificant. Substantial thermalization of ions occurs as gyrating ions are observed at the steepened edge. These observations indicate that the mechanisms causing the dissipation of magnetic fields (currents) and ions are different in the early phase of shock development.

DOI: 10.1103/PhysRevLett.103.031101 PACS numbers: 96.50.Ci, 52.35.Mw, 52.35.Tc, 96.50.Fm

Understanding how collisionless shocks form in nature is one of the most important problems in space and astrophysics. Many observations since the discovery of Earth's bow shock in the 1960s [1] have revealed that shocks can form in collisionless plasmas and nonlinear processes are important in their formation. An interesting feature of collisionless shocks is that the length scale of the transition layer is much shorter than the collisional mean free path. Macroscopic thermalization is mediated by microscopic dissipation processes within the layer. However, the physical processes of how shocks form in collisionless plasmas still remain poorly understood.

Various kinds of nonlinear phenomena have been observed in regions upstream of Earth's bow shock [2]. They include hot flow anomalies [3,4], foreshock cavities [5], short large-amplitude magnetic structures [6], and density holes (DHs) [7–9]. These structures share some common features, but each also has unique features. The generation mechanisms of these structures and their relationships are still under investigation. Frequently observed in these structures are greatly enhanced edges that have properties similar to shocks [7,10–12]. The transient nature of these structures suggests the edges are growing nonlinearly and ending up as shocks. Investigation of these structures can thus yield important clues about how shocks develop in collisionless plasmas. However, until recently measurements of the temporal development of nonlinear structures in space have been limited.

The Cluster mission [13] provides an opportunity for greatly improved *in situ* measurements of the temporal development. During the apogee passes in the solar wind in 2003, the Cluster spacecraft were aligned predominantly along the Sun-Earth line with the separation as large as $\sim 1.6\,R_E$ (radius of Earth). This configuration has enabled us to observe the temporal development of structures moving with the solar wind as it passes by the spacecraft. Here we present first *in situ* observations that demonstrate nonlinear steepening of compressional pulses and formation of shocklike structures.

The magnetic fields [14] from the four Cluster spacecraft show a steepening event observed on 16 February 2003 (Fig. 1). At ~1050 UT Cluster 1 (SC1) was in the solar wind at $\sim(9.8, -1.5, -9.7)\,R_E$ in geocentric solar ecliptic coordinates, and separated from SC4 in the X, Y,

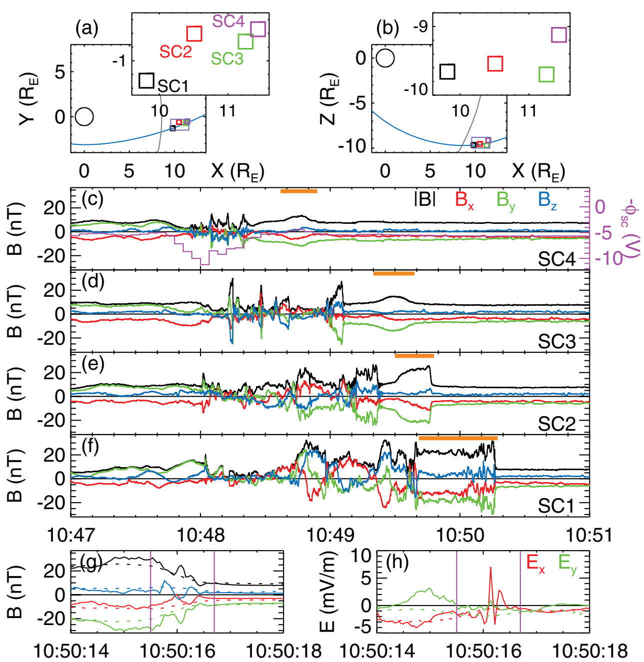

FIG. 1 (color). Orbit of the Cluster spacecraft projected onto the (a) xy and (b) xz planes in the geocentric solar ecliptic coordinates on 16 February 2003 (blue line). Shown in included boxes is the configuration of the Cluster spacecraft at 1050 UT. The gray curve represents the model bow shock location. Magnetic field measurements are shown from (c) to (f). Full resolution (22.5 Hz) data were used. The compressional pulse and shocklike structure are marked by the orange bar. Spacecraft potential, $-\phi_{sc}$, is also plotted in (c). Bottom panels show (g) magnetic and (h) electric fields measured by SC1 (solid lines) and SC2 (dotted lines). The time on SC2 was shifted by 30 s to match the edges.

and Z directions by $\sim$1.6, $\sim$0.75, and $\sim$0.58 R_E, respectively. Cluster was moving earthward, and SC1 encountered the bow shock at $\sim$1210 UT at $\sim$(8.4, $-$1.8, $-$9.7) R_E (not shown).

A DH was observed on SC4 between $\sim$1047:50 and $\sim$1048:20 UT. It is identified by a depression in $|\mathbf{B}|$ and the spacecraft potential, $-\phi_{sc}$, which is a proxy for electron density [7,9]. A compressional pulse was observed at the upstream edge of the DH [~1048:45 UT, marked by the orange bar in Fig. 1(c)]. The amplitude of the pulse, $\delta B/B_0$, was $\sim$0.84, where B_0 is the magnitude of the upstream B field and δB is the enhancement at the pulse. Subsequent observations from the other spacecraft indicate the DH developed in a complicated way, including large-amplitude peaks [e.g., between $\sim$1048:00 and $\sim$1049:05 UT in Fig. 1(d)]. In this Letter, we focus only on the development of the compressional pulse observed at the upstream edge of the DH (marked by the orange bars in Fig. 1).

On SC3 $\delta B/B_0$ increased slightly to $\sim$0.95, indicating growth without change in shape. On SC2, however, the amplitude has more than doubled, $\delta B/B_0 \sim 2.4$. The estimated average growth rate $\Delta(\delta B/B_0)/\Delta t$ between SC4 and SC3 is $\sim$0.0024 s^{-1}, while between SC3 and SC2, $\Delta(\delta B/B_0)/\Delta t \sim 0.097$ s^{-1}, $\sim$40 times larger. Thus, the pulse grew impulsively between SC3 and SC2. Moreover, the edge of the pulse facing the solar wind (~1049:45 UT) sharply steepened. Because the separation between SC2 and SC3 was mainly along the X direction ($\Delta X \sim 0.75$, $\Delta Y \sim 0.11$, and $\Delta Z \sim 0.16\, R_E$) and the structure was moving in the X direction embedded in the solar wind, it is reasonable to assume that a similar plasma region was sampled by SC2 and SC3. Thus, the variations observed from SC3 to SC2 can be interpreted consistently as growing and breaking of a nonlinear pulse.

On SC1 it is possible to see that the pulse had developed into a shocklike structure with a ramp, overshoot, and a magnetosheath-like downstream region. The amplitude was comparable to that on SC2, indicating that after steepening the amplitude ceased to grow. Figures 1(g) and 1(h) show an expanded view of B and electric (E) fields [15] measured on SC1 (solid lines) and SC2 (dotted lines; shifted by 30 s to match the edge) across the edge. On SC1, a few Hz frequency oscillations occurred across the edge (within vertical bars) in both B and E fields, while the transition on SC2 was smooth. These embedded oscillations may be an early phase of whistler mode waves or electromagnetic oscillations that could propagate to the upstream region of shocks [16,17].

Figure 2 shows ion measurements by the hot ion analyzer (HIA) instrument [18] made on SC3 and SC1. The narrow, intense band centered at $\sim$2 keV in the energy flux spectrogram after $\sim$1050 UT on SC3 represents the solar wind ion beam. The DH, observed between $\sim$1048:00 UT and $\sim$1049:10 UT on SC3, appears as a broad diffuse spectrum with low density and high temperature. The spectrogram shows that the pulse on SC3 consisted of a slightly broadened solar wind ion beam. A sharp boundary at $\sim$1049:10 UT separates the diffuse ions inside the DH from the beam at the pulse, but there is no such clear boundary distinguishing the solar wind from the pulse. On the other hand, on SC1 a discernible boundary was formed at $\sim$1050:15 UT, separating the broader spectrum of ions in the shocklike structure from the narrow solar wind beam. Although broader than that on SC3 [Fig. 2(j)], the phase space distribution of ions in the shocklike structure was still beamlike [Fig. 2(k)], clearly distinguishable from the isotropic distribution in the DH [Fig. 2(i)]. No gyrating ions were observed. Examination of the electric field shows the cross-shock potential is much less than the

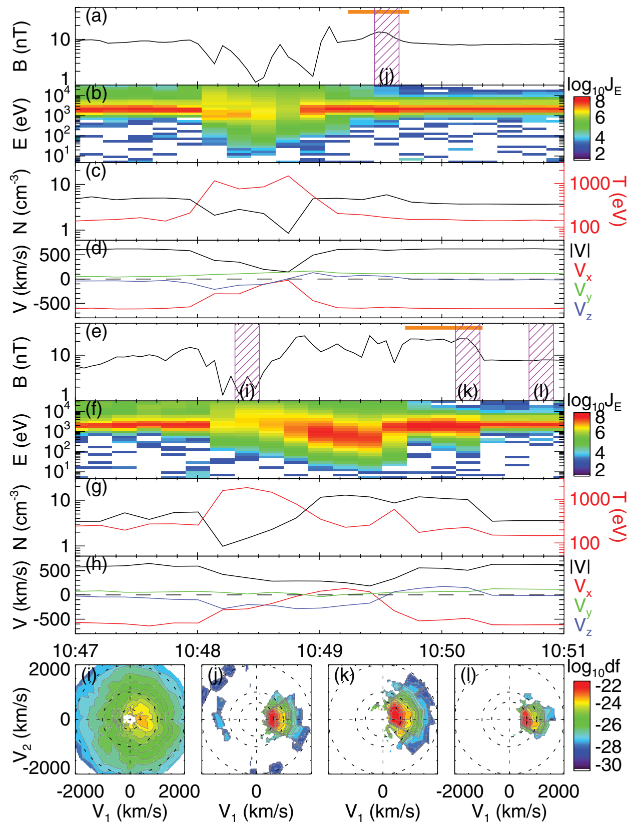

FIG. 2 (color). Ion measurements by HIA on 16 February 2003. The top four panels (a–d) represent the measurements by SC3, and next four panels (e–h) by SC1. In each set of four panels, shown from top to bottom are the magnitude of the magnetic field, ion energy flux spectrogram integrated over all directions, density and temperature, and velocity moments. Ion moments were calculated from the three-dimensional distributions with 12 s resolution. The bottom panels show ion velocity space distributions, from left to right, (i) in the DH, (j) at the pulse, (k) in the shocklike structure, and (l) in the upstream solar wind. The times that the distributions are obtained are marked by hatched regions in (a) and (e). V_1 and V_2 are along $\mathbf{V}$ (velocity moment) and $\mathbf{V} \times \mathbf{B}$, respectively (chosen to capture both the solar wind and gyrating ions).

kinetic energy of incident ions, which is consistent with the absence of gyrating ions. Across the edge the temperature only slightly increased from ~150 to ~230 eV. Thus, even though the pulse steepened and became shocklike, the heating of the ions in the shocklike structure was very small.

The boundary normal, **n**, of the shocklike edge (~1050:15 UT) was estimated using the Abraham-Shrauner method [19], which is reliable for oblique and perpendicular shocks [20]. This yielded $\mathbf{n} \sim (0.45, -0.14, 0.88)$, whose angle to the upstream B field, $\theta_{\rm Bn}$, was ~81°. Assuming the initial DH as a tangential or rotational discontinuity, the boundary normal of the DH on SC4 $(\mathbf{B}_u \times \mathbf{B}_d / |\mathbf{B}_u \times \mathbf{B}_d|)$ was estimated as $\mathbf{n} \sim (0.18, 0.053, 0.98)$. The orientations of the two normal vectors differ only by ~20°, suggesting that the shocklike structure formed along the DH. The speed of the steepened edge along the normal direction in the spacecraft frame, determined by the continuity of the tangential electric field, was $V_n \sim -16$ km/s, much less than the solar wind speed. The solar wind ions could not pass through the DH, but were slowed down or deflected around the DH [7,9]. Thus, the DH acted as a barrier for the formation and steepening of the pulse. However, how the DH stands against the solar wind is not yet understood. The estimated thickness of the edge (ramp) is ~33 km, which is less than both the ion inertial length ($r_i \sim 93$ km) and the gyroradius of protons with temperature of ~150 eV ($r_g \sim 230$ km) in the upstream solar wind. Note that the estimation of normal speed and thickness can have errors because ideal situations, e.g., plane boundary and constant speed, were assumed. However, the errors do not substantially change the interpretations. The upstream Alfvén and fast magnetosonic Mach numbers were ~4.5 and ~2.1, respectively, and plasma β was ~1.8. The shocklike structure could be in a turbulent regime of shock classification, observed as the low-frequency oscillations across the steepened edge.

Another event was observed on 12 March 2003 (Fig. 3). Initially SC1 and SC2 were in the magnetosheath while SC3 and SC4 were in the solar wind. Because the bow shock moved earthward, SC1 and SC2 moved into a region that was originally a DH but highly disturbed while interacting with the bow shock. On SC4 a DH, which was already disturbed, was observed between ~0230 and ~0231 UT. An amplified, shocklike structure had already formed at the upstream edge (~0231:10 UT, marked by the orange bar) of the DH with $\delta B/B_0 \sim 1.5$. Thus, this event could be in a more developed state than the previous one. On SC3 $\delta B/B_0$ increased slightly to ~2.0, and remained similar on SC2 and SC1, which is consistent with the previous event that the amplitude ceases to grow after steepening. Instead, the downstream region (orange bars) was largely expanded from SC4 to SC1. Fully developed overshoot was observed on SC1 accompanied by intense high frequency whistler mode waves. Lacking nested features, the sequence of the shocklike structure observed from SC4 to SC1 did not result from back and forth motion of the bow shock, but an earthward motion of the structure with the solar wind.

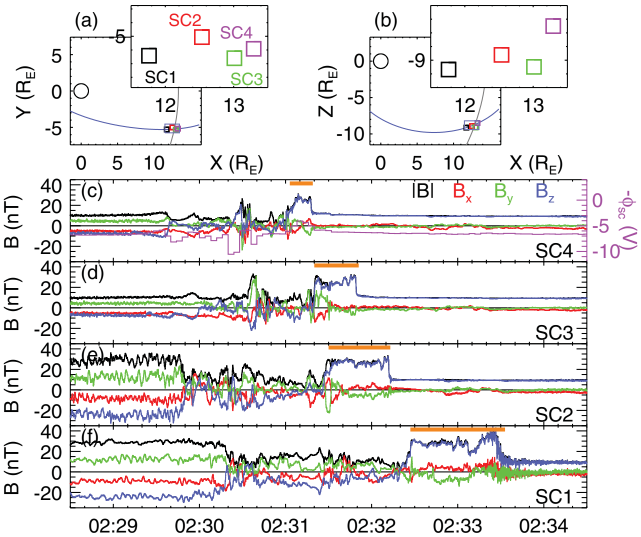

FIG. 3 (color). (a) and (b) Orbit and configuration (at 0230 UT) of the Cluster spacecraft on 12 March 2003 [same format as Figs. 1(a) and 1(b)]. Magnetic field measurements on 12 March 2003 are shown from (c) to (f) (22.5 Hz resolution). The shocklike structure is marked by the orange bar. Spacecraft potential, $-\phi_{\rm sc}$, is also plotted in (c).

Figure 4 shows the ion measurements from SC1 (SC3 was in a mode that was not suitable for this study). Interacting with the bow shock (~0230:20 UT), the DH developed into a hot, dense region appearing as broad

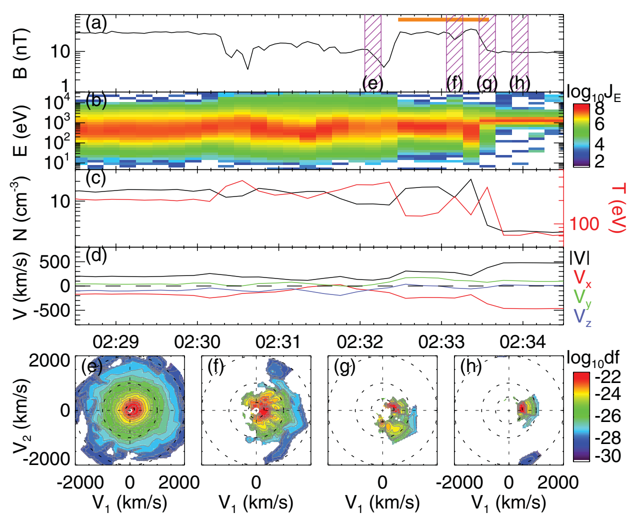

FIG. 4 (color). Ion measurements by HIA on board SC1 on 12 March 2003. The top four panels are in the same format as Figs. 2(a)–2(d). The bottom panels show ion velocity space distributions, from left to right, (e) in the DH, (f) in the shock downstreamlike region, (g) at the edge of the shocklike region, and (h) in the upstream solar wind [same format as Figs. 2(i)–2(l)].

diffuse spectra between ~0230:20 and ~0232:30 UT. The shocklike structure between ~0232:30 and ~0233:30 UT consisted of ions with broader spectra than the solar wind, but narrower than the diffuse ions in the disturbed DH and magnetosheath. The phase space distribution at the steepened edge shows two distinguishable populations: beamlike and gyrating populations [Fig. 4(g)]. The beamlike ions are similar to the solar wind [Fig. 4(h)]. The gyrating ions are seen in the lower half sector of the phase space ($V_2 < 0$) in Fig. 4(g). The presence of gyrating ions at the shock ramp is one of the characteristics of supercritical, quasiperpendicular shocks [21]. Further inside the downstream region, the distribution became highly dispersed and jagged [Fig. 4(f)]. This could be due to multiple gyrating beams [22] and indicate strong instabilities had been occurring in the shocklike structure thermalizing the ions. Note, however, the distribution is still distinguishable from the hot, isotropic distributions in the DH [Fig. 4(e)] and magnetosheath (not shown). The density varied almost identically with $|\mathbf{B}|$, while the temperature substantially increased from ~71 to ~300 eV from the foot of the steepened edge, where $|\mathbf{B}|$ and the density were still low. This implies that nonadiabatic heating was produced at the edge. The gyrating ions are responsible for the nonadiabatic heating [23,24].

The normal of the edge was estimated as $\mathbf{n} \sim (0.95, -0.088, -0.30)$, and $\theta_{\rm Bn} \sim 63°$. The speed of the edge was $V_n \sim -41$ km/s. The thickness was ~280 km, which is greater than both the ion inertial length ($r_i \sim$ 93 km) and the gyroradius of protons with temperature of ~71 eV ($r_g \sim 130$ km). The thickness of the edge on SC1, which was the latest in time, was larger than that on the other spacecraft. The intense whistler mode waves observed only on SC1 may be responsible for the larger thickness of the edge by making it more diffuse. Previous studies have reported that the thickness of the ramp for low Mach number shocks is approximately the ion inertial length, while for high Mach number shocks it is proportional to the gyroradius of upstream ions [25,26]. The upstream Alfvén and fast magnetosonic Mach numbers were ~4.7 and ~3.7, respectively, and plasma β was ~0.71.

These observations show that shocks can form by nonlinear steepening of compressional pulses in collisionless space plasmas. In the early phase of the development a compressional pulse formed at the upstream edge of a DH slowly grows. However, after a certain point the pulse amplifies "explosively," and the edge facing the solar wind sharply steepens. After the steepening, the amplification ceases, but the downstream region starts to expand. One of the important features is that the steepening can occur without significant thermalization of ions, suggesting different processes are involved in the dissipation of magnetic fields (currents) and ions in the pulses. Substantial thermalization of ions occurs when gyrating ions are observed. The occurrence of the gyrating ions is related to the cross-shock potential and the thickness of the steepened edge. Right after steepening, the thickness of the edge is smaller than the ion inertial scale. Also, the cross-shock potential is much smaller than the kinetic energy of incident ions. Thus, the incident ions just pass through the edge without gyration. Dissipation at the edge increases the thickness for gyrating ions, which subsequently excite instabilities and thermalize ions [23]. The sharp steepening of the edge without involving ions in the early development suggests that the processes with finer scales than ion dynamics scales are important on the steepening of the pulse. Thus, electron dynamics can be important in the early development of shocks.

This work was supported by NASA Grants No. NNG04GF23G and No. NNG05GF99G. The authors thank the Cluster CIS, FGM, and EFW teams and the Cluster Active Archive for providing the data.

*eslee@ssl.berkeley.edu

[1] N. F. Ness, C. S. Scearce, and J. B. Seek, J. Geophys. Res. **69**, 3531 (1964).
[2] J. P. Eastwood *et al.*, Space Sci. Rev. **118**, 41 (2005).
[3] S. J. Schwartz *et al.*, Nature (London) **318**, 269 (1985).
[4] M. F. Thomsen *et al.*, J. Geophys. Res. **91**, 2961 (1986).
[5] D. G. Sibeck *et al.*, J. Geophys. Res. **107**, 1271 (2002).
[6] S. J. Schwartz *et al.*, J. Geophys. Res. **97**, 4209 (1992).
[7] G. K. Parks *et al.*, Phys. Plasmas **13**, 050 701 (2006).
[8] N. Lin *et al.*, Ann. Geophys. **26**, 3707 (2008).
[9] M. Wilber *et al.*, Ann. Geophys. **26**, 3741 (2008).
[10] S. A. Fuselier *et al.*, J. Geophys. Res. **92**, 3187 (1987).
[11] S. J. Schwartz and D. Burgess, Geophys. Res. Lett. **18**, 373 (1991).
[12] E. A. Lucek, T. S. Horbury, and A. Balogh, J. Geophys. Res. **109**, A06207 (2004).
[13] C. P. Escoubet, M. Fehringer, and M. L. Goldstein, Ann. Geophys. **19**, 1197 (2001).
[14] A. Balogh *et al.*, Ann. Geophys. **19**, 1207 (2001).
[15] G. M. Gustafsson *et al.*, Ann. Geophys. **19**, 1219 (2001).
[16] C. T. Russell, J. Atmos. Sol. Terr. Phys. **69**, 1739 (2007).
[17] M. N. Nozdrachev, A. A. Petrukovich, and J. Juchniewicz, Ann. Geophys. **13**, 573 (1995).
[18] H. Réme *et al.*, Ann. Geophys. **19**, 1303 (2001).
[19] B. Abraham-Shrauner, J. Geophys. Res. **77**, 736 (1972).
[20] A. F. Viñas and J. D. Scudder, J. Geophys. Res. **91**, 39 (1986).
[21] G. Paschmann *et al.*, Geophys. Res. Lett. **9**, 881 (1982).
[22] N. Sckopke *et al.*, J. Geophys. Res. **88**, 6121 (1983).
[23] D. Burgess, W. P. Wilkinson, and S. J. Schwartz, J. Geophys. Res. **94**, 8783 (1989).
[24] N. Sckopke *et al.*, J. Geophys. Res. **95**, 6337 (1990).
[25] C. T. Russell *et al.*, Geophys. Res. Lett. **9**, 1171 (1982).
[26] S. D. Bale, F. S. Mozer, and T. S. Horbury, Phys. Rev. Lett. **91**, 265004 (2003).